Joint Special Interest Group meeting between euspen and ASPE
Advancing Precision in Additive Manufacturing
Ecole Centrale de Nantes, France, September 2019
www.euspen.eu

Experimental analysis of the filament feeding force in material extrusion additive manufacturing

Marcin P. Serdeczny[1], Raphaël Comminal[1], David B. Pedersen[1], Jon Spangenberg[1]

[1]Department of Mechanical Engineering, Technical University of Denmark, Kgs. Lyngby, Denmark

mpse@mek.dtu.dk

Abstract
In this study, the force required to feed the solid filament through the nozzle in material extrusion additive manufacturing was measured and analysed. The filament is a source of the building material in this process, but also acts as a piston to drive the flow of the molten polymer. Thus, the filament feeding force relates to the pressure inside the nozzle and the flow conditions, which are not well understood yet, due to the complex rheology of polymers. An experimental setup was designed and built to measure the filament feeding force at different extrusion temperatures and flow rates. It was observed that at high feeding rates, the force starts to oscillate, indicating pressure fluctuations in the flow, which could be due to viscoelastic phenomena of the molten polymer or oscillating length of the melt zone inside the liquefier. Moreover, the pressure fluctuations were accompanied by the fluctuations in the extrudate swelling, which might lead to a degradation of the geometrical quality of the prints. These effects must be understood in order to maintain manufacturing precision when increasing the building rates in future material extrusion additive manufacturing machines.

Material extrusion additive manufacturing, experimental measurements, extrusion force, polymer flow

1. Introduction

In material extrusion Additive Manufacturing (AM), also known as Fused Filament Fabrication (FFF) and Fused Deposition Modelling (FDM), a solid filament is used to supply the building material, and to generate the pressure inside the liquefier and the extrusion nozzle (together called the *hot-end*). The filament is fed by one or two gear wheels that are driven by a stepper motor (the *cold-end*), which is controlled in an open loop system. The filament, made of polymer, is melted in the hot-end and extruded layer by layer to create a 3D object. The extrusion temperature is usually controlled with a PID loop using a thermistor mounted inside the liquefier that provides the only feedback about the flow conditions inside the hot-end, in most of the machines.

The simple design and low cost of material extrusion AM machines is one of the reasons for their success on the market. However, the lack of closed-loop control makes the choice of printing parameters a crucial step in achieving desired properties of the produced component. This is very challenging due to complex physical phenomena that govern the process. In particular, the melting and the flow of polymer through the liquefier is not well understood yet in the literature, as discussed in [1,2]. For instance, as the inverse function of the liquefier response to a change of the feeding rate is generally unknown, it is impossible to predict extrusion rate at transient states, which are very common during the process due to additive nature (object is manufactured by printing short segments). The extrusion rate determines shapes of the printed stands and therefore macroscopic properties of the part [3–6].

Furthermore, among major limitations to increase the building rates in material extrusion AM, are the filament feeding mechanism and the rate of heat transfer inside the hot-end [7]. The first limitation relates to the magnitude of force that needs to be applied to the filament in order to overcome the pressure drop in the extrusion nozzle. The rate of heat transfer determines how quickly the filament will be melted without overheating and degrading the polymer. In essence, both of these limitations also relate to the fluid dynamics of molten polymer in the extrusion nozzle.

The flow phenomena governing the process can be understood through a careful analysis of the conditions inside the hot-end. Phan et al. [8] estimated the pressure inside the nozzle based on the power delivered to the stepper motor. Anderegg et al. [2] used a pressure transducer mounted inside the nozzle and reported pressures for different extrusion temperatures. Coogan and Kazmer [9] presented a nozzle design with an in-situ rheometer that monitors the melt viscosity during the process. In these studies, an effort was made to investigate the steady state values of the pressure inside the hot-end.

In this work, we present an experimental setup to measure the force required to push the filament through the hot-end. This force directly relates to the total pressure drop through the hot-end and informs about the flow conditions during the process. The feeding force is analysed as a function of time and is related to the appearance and swell of the extrudate. Section 2 describes the experimental setup and experiments. The results of the study are presented and discussed in Section 3. Conclusions are given in Section 4.

2. Experimental setup

2.1. Filament feeding force measurements

Figure 1 presents the experimental setup used in this study to measure the filament feeding force. The extrusion has been isolated from the deposition by keeping the nozzle away from the substrate. The setup was equipped with (1) a BondTech QR extruder that differs from many extruders by having two gear wheels to drive the filament, providing twice as much area to

apply the feeding force; (2) an E3D v6 hot-end with a nozzle diameter of D = 0.4 mm; (3) a RAMPS v1.4 3D printer controller; (4) a 20 kg load cell with a HX711 interface; (5) an Arduino Mega controller board as a data acquisition device; (6) a 12 V power supply; (7) PLA filament with a diameter D_f = 1.75 mm. Both the RAMPS v1.4 (3) and the Arduino (5) were connected to a PC via USB. The extruder (1), and the hot-end (2) were controlled using Marlin firmware [10] and Pronterface [11], which allows online command of the 3D printer. The measurement data were acquired using Matlab. The load cell and liquefier temperature readings were recorded with an average frequency of 10 Hz. In order to reduce any noised present in the signal, a moving average over last five readings was used during the measurement.

Before the experiments, the PID controller of the heating block was tuned using an internal Marlin procedure. Then, the extruder control was adjusted to ensure the correct nozzle throughput. The adjustment was done by changing the number of stepper motor steps per mm in the firmware, until the requested length of the filament was fed with an accuracy of 0.5 %. The uncertainty of the force measurement is estimated as a 0.1 % of the total scale of the load cell i.e. 20 kg. Hence, uncertainty of the force measurement was around 0.2 N. One side of the load cell was fixed to the extruder and the other one to the hot-end, similarly as in [7], allowing bending of the load cell under the feeding force.

As previously mentioned, the feeding force is related to the pressure inside the liquefier. The molten polymer is pushed by the solid filament, which generates the feeding pressure P as

$$P = \frac{F}{A} = \frac{4F}{\pi D_f^2}$$

where F is the filament feeding force, A is the filament cross-sectional area, and D_f is the filament diameter.

Each experiment consisted of extruding the material for 60 s at a fixed feeding rate and extrusion temperature T_s. The first 30 s of each measurement were disregarded as they contained transient adjustment of the flow. The average and standard deviation of the feeding force and the liquefier temperature where calculated from the last 30 s of the experiments. Moreover, for each tested printing condition, the measurements were repeated three times and the average $\bar{F}$ and standard deviation of the force $\sigma(\bar{F})$ were calculated from those three trials. Additionally, the average of the standard deviations $\overline{\sigma(F)}$ with respect to time were calculated, representing variations of the feeding force in time within a single measurement. The same was done for the calculated pressure. The feeding rate V was varied from 0.66 mm/s (40 mm/min) with increments of 0.33 mm/s (20 mm/min) until the required feeding force was so large that the driving wheels started to grind the filament.

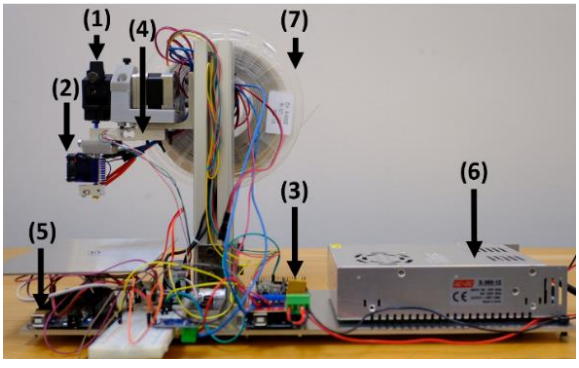

Figure 1. Picture of the experimental setup (see description in the text).

2.2. Extrudate swell measurements

A digital camera was used to record the swelling of the extruded material. In most of the tested extrusion conditions, the flow reached a steady state and the swell could be measured with a single photograph during the extrusion. However, for high filament feeding rates, the swell was varying in time and a movie was recorded. The recorded pictures and movies were later post-processed in Matlab using image recognition. The contours of the extruded strands were detected and the extrudate diameter D_e was calculated in multiple points along the strand. Next, the results were averaged and normalized by the nozzle diameter D to obtain the swell ratio S_r. The uncertainty of the method is estimated by the standard deviation of the measurements of the extrudate diameter (at printing conditions when no fluctuations in the swell were present, i.e. the lowest feeding rates). The measured uncertainty of D_e was around 10 µm.

3. Results and discussions

Figure 2 presents measurements of the feeding force, feeding pressure (top), and the liquefier temperature (bottom) during the extrusion, at different filament feeding rates F and the extrusion set-point temperature T_s = 200 °C. For each printing condition, one of the three conducted measurements is shown, however the presented analysis is true for all three repetitions. Figure 3 presents selected photographs of the extruded material at chosen feeding rates and set-point temperatures. In Figure 2, we can see that the feeding force is relatively constant for low filament feeding rates. When the feeding rate is increased, small oscillations of the force are visible, however no significant periodic changes in the temperature or the diameter of the extruded strand were observed (see Figure 3; left). These force (and pressure) oscillations in time are quantified by the means of the standard deviations ($\overline{\sigma(F)}$ and $\overline{\sigma(P)}$), and are reported in Table 1. It is observed that, when changing the filament feeding rate from V = 1.7 mm/s to V = 3 mm/s, the standard deviation of the measured force increases twofold, while when increasing from V = 3 mm/s to V = 4.3 mm/s, the standard deviation increases over 10 times, which is due to the observed force oscillations. Further increase of the feeding rate caused failure in the material extrusion, when the required feeding force exceeded the filament material strength. For that case, the time trace of the feeding force was shown with a dashed line in Figure 2. The extrusion failed at a feeding force of around 150 N (60 MPa), which is around twice as high as reported in [7], however it is noted that the extruder used in the present study has gear wheels on both sides of the filament providing around twice as much of contact area to apply the force. By looking at Table 1, it can be seen that during the normal operation in material extrusion AM, the feeding force will be in the range from 5 N to 15 N, while corresponding pressure between 1 MPa and 6 MPa, However at high feeding rates the pressure can reach values as high as 30 MPa.

In order to investigate the feeding force at higher flow rates, the liquefier temperature was increased to 250 °C. This reduced the viscosity of the molten polymer and the required feeding force, as it can be seen in comparison of Figure 4 (T = 250 °C) to Figure 2 (T = 200 °C), and in Table 1. Moreover, we observed less extrudate swelling when T = 250 °C (see: Figure 3, middle; and Table 1). Interestingly, at V = 6.7 mm/s, high frequency oscillations are seen in the measurement of the force, while periodical changes are also observed in the diameter of the extruded strand (Figure 3; right). By investigating bottom plot of Figure 4 and Table 1, it can be seen that variations in the liquefier temperature are independent of the feeding rate.

Table 1. Statistics of the measurements of the filament feeding force, pressure, liquefier temperature, and swell ratio of the extrudate.

No	Feeding Rate	Flow Rate	Set-point temperature	Feeding Force			Feeding Pressure			Liquefier temperature			Swell ratio
	V	Q	T_s	$\bar{F}$	$\sigma(\bar{F})$	$\overline{\sigma(F)}$	$\bar{P}$	$\sigma(\bar{P})$	$\overline{\sigma(P)}$	$\bar{T}$	$\sigma(\bar{T})$	$\overline{\sigma(T)}$	$\overline{S_r}$
	mm/s	mm3/s	°C	N	N	N	MPa	MPa	MPa	°C	°C	°C	-
1	1.7	4.0	200	7.5	0.4	0.1	3.1	0.15	0.06	200	0.1	0.5	1.2
2	3.0	7.2	200	13.6	0.4	0.2	5.7	0.15	0.10	200	0.1	0.5	1.4
3	4.3	10.4	200	67.7	1.2	2.6	28.2	0.51	1.08	200	0.1	0.5	2.7
4	5.0	12.0	200	49.1	n/a	37.9	20.4	n/a	15.7	200	n/a	0.5	n/a
5	1.7	4.0	250	2.5	0.1	0.2	1.1	0.03	0.08	250	0.1	1.3	1.0
6	3.0	7.2	250	4.7	0.2	0.2	1.9	0.08	0.07	250	1.5	1.3	1.1
7	4.3	10.4	250	9.1	0.4	0.2	3.8	0.19	0.09	249	0.2	1.3	1.6
8	5.0	12.0	250	16.4	0.3	0.9	6.8	0.13	0.36	249	0.1	1.1	1.6
9	6.7	16.0	250	81.0	1.8	6.4	33.7	0.75	2.65	249	0.1	1.2	3.2
10	7.7	18.4	250	76.2	n/a	33.7	31.7	n/a	14.0	249	n/a	1.4	n/a

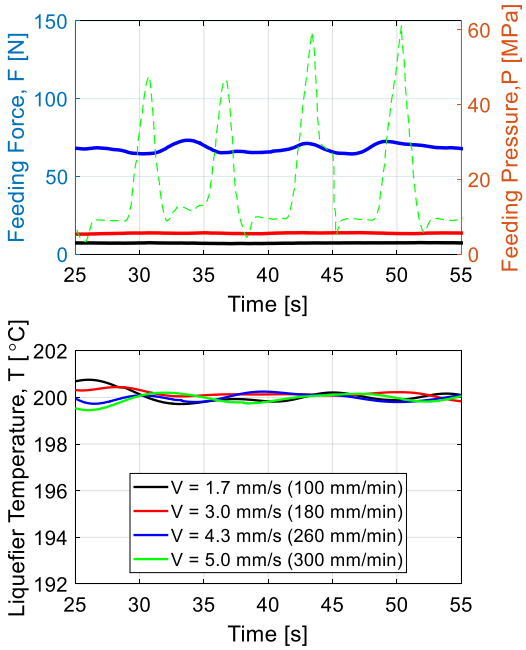

Figure 2. Measurement of the feeding force (top) and liquefier temperature (bottom) for different filament feeding rates and extrusion temperature 200 °C. The force measurement when feeding mechanics failed by grinding the filament is shown with dashed line.

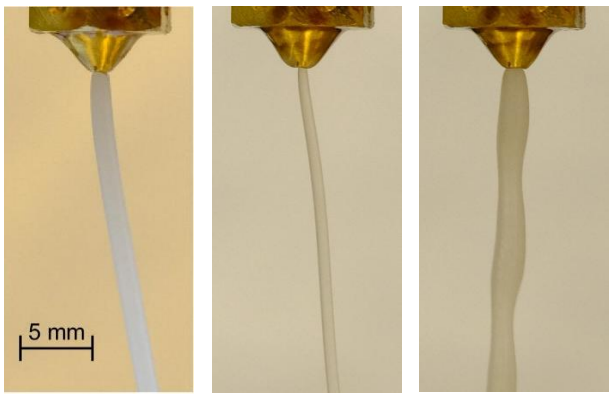

Figure 3. Appearance of the extruded strand at different filament feeding rates and temperatures

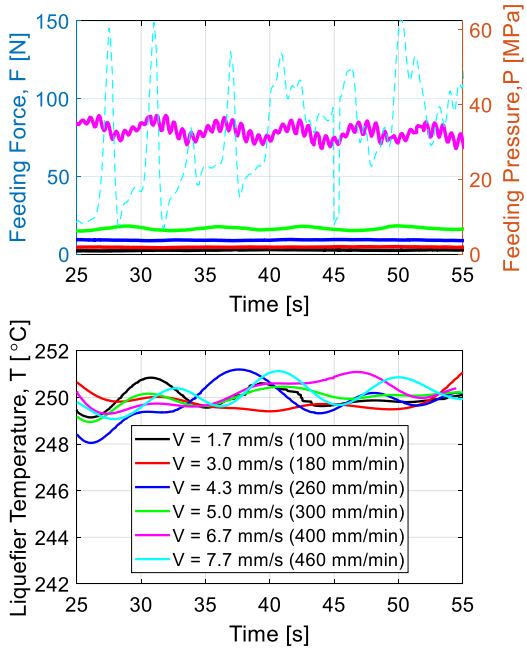

Figure 4. Measurement of the feeding force (top) and liquefier temperature (bottom) for different filament feeding rates and extrusion temperature 250 °C. The force measurement when feeding mechanics failed by grinding the filament is shown with dashed line.

This indicates that the force oscillations are rather not caused by a failure in the heating block control. However, possible explanation of the force oscillations can be due to fluctuating temperature of the polymer melt, which may not be reflected in the liquefier thermistor readings. The pressure build-up can create a backflow of the molten polymer that increases the area of contact between the polymer and the liquefier. This, in return, would cause the temperature to increase, the melt viscosity to decrease, and pressure to drop again. The force oscillations could also be caused by the pressure fluctuations due to periodic viscoelastic phenomena of the polymeric flow [12,13]. Regardless of which mechanism is responsible for the observed phenomena, the pressure fluctuations will cause backflow inside the nozzle, and oscillating extrusion rate. Hence, observed variations in the extrude swell. Further increase of the feeding rate led again to the grinding of the filament, which is seen as the large drops of the measured force (dashed line).

In the end, we look at the relation between the aforementioned oscillations in the feeding force and the swell ratio of the extrudate. In Figure 5, the time traces (top) and power spectral densities (bottom) of the swell measurements are shown for the extrusion conditions, at which oscillations in the filament feeding force occurred. Fluctuations in the extrude swell were clearly visible in two out of three measurements for which feeding force oscillations were observed (see Figure 2 and Figure 4). By looking at the power spectral densities of the swell measurement and the filament feeding force shown in Figure 6, it can be seen that periodic fluctuations in the swell and the force occur with the same frequency. For V = 5.0 mm/s (T_s = 250 °C), the peaks in the power density of the swell and the force occur at around 0.2 Hz. For V = 6.7 mm/s (T_s = 250 °C), the swell and force oscillations have lower and higher frequency components, i.e. at 0.2 Hz and 1.5 Hz. This indicates that these oscillations are related, and perhaps due to the same physical mechanisms, as discussed previously.

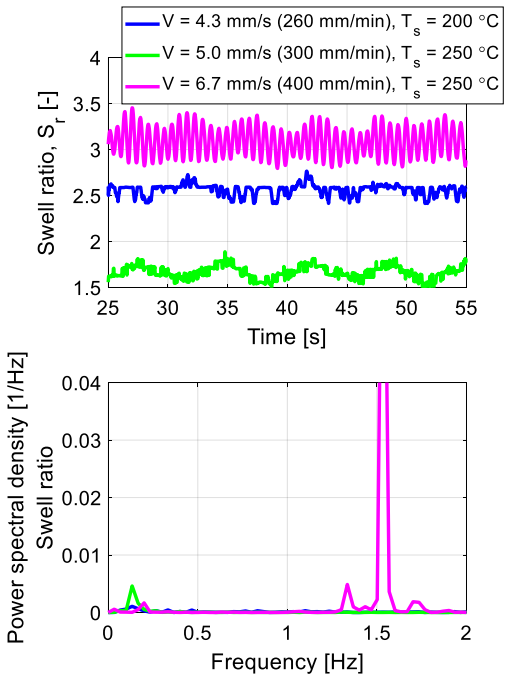

Figure 5. Measurements of the swell ratio in time (top) and power spectral density of the signal (bottom). Measurements shown only for the extrusion conditions, for which oscillations in the feeding force occurred.

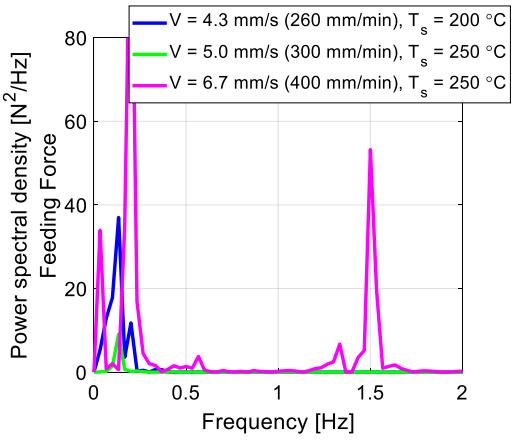

Figure 6. Power spectral density of the filament feeding force for three highest feeding rates, for which oscillations in the signal occurred.

4. Conclusions

We designed an experimental setup to measure the filament feeding force in material extrusion additive manufacturing. It was shown that the force starts to oscillate at high filament feeding rates, which may be caused by the fluctuations in the length of the melt zone inside the liquefier or periodic viscoelastic phenomena of the molten polymer, as we also observed fluctuations in the extrudate swelling. These fluctuations of the extrudate swelling could negatively influence the geometrical quality of the manufactured component. More importantly, understanding the dynamics of the polymer flow inside the liquefier is essential for the development of reliable control methods of material extrusion AM. Therefore, further work is required to understand completely the physical phenomena behind this process. Additionally, with increasing building rates in material extrusion AM, design of new machines will need to account for the investigated effects.

Acknowledgements

The authors would like to acknowledge the support of the Danish Council for Independent Research (DFF) | Technology and Production Sciences (FTP) (Contract No. 7017-00128).

References

[1] Mackay ME. The importance of rheological behavior in the additive manufacturing technique material extrusion. *J Rheol* (N Y N Y) 2018;**62**:1549–61. doi:10.1122/1.5037687.

[2] Anderegg DA, Bryant HA, Ruffin DC, Skrip SM, Fallon JJ, Gilmer EL, et al. In-situ monitoring of polymer flow temperature and pressure in extrusion based additive manufacturing. *Addit Manuf* 2019;**26**:76–83. doi:10.1016/j.addma.2019.01.002.

[3] Comminal R, Serdeczny MP, Pedersen DB, Spangenberg J. Numerical modeling of the strand deposition flow in extrusion-based additive manufacturing. *Addit Manuf* 2018;**20**:68–76. doi:10.1016/j.addma.2017.12.013.

[4] Serdeczny MP, Comminal R, Pedersen DB, Spangenberg J. Experimental validation of a numerical model for the strand shape in material extrusion additive manufacturing. *Addit Manuf* 2018;**24**:145–53. doi:10.1016/j.addma.2018.09.022.

[5] Serdeczny MP, Comminal R, Pedersen DB, Spangenberg J. Numerical simulations of the mesostructure formation in material extrusion additive manufacturing. *Addit Manuf* 2019;**28**:419–29. doi:10.1016/j.addma.2019.05.024.

[6] Comminal R, Serdeczny MP, Pedersen DB, Spangenberg J. Motion planning and numerical simulation of material deposition at corners in extrusion additive manufacturing. *Addit Manuf* 2019. doi:10.1016/j.addma.2019.06.005.

[7] Go J, Schiffres SN, Stevens AG, Hart AJ. Rate limits of additive manufacturing by fused filament fabrication and guidelines for high-throughput system design. *Addit Manuf* 2017;**16**:1–11. doi:10.1016/j.addma.2017.03.007.

[8] Phan DD, Swain ZR, Mackay ME. Rheological and heat transfer effects in fused filament fabrication. *J Rheol* (N Y N Y) 2018;**62**:1097–107. doi:10.1122/1.5022982.

[9] Coogan TJ, Kazmer DO. In-line rheological monitoring of fused deposition modeling. *J Rheol* (N Y N Y) 2018;**63**:141–55. doi:10.1122/1.5054648.

[10] Home | Marlin Firmware n.d. http://marlinfw.org/ (accessed June 18, 2019).

[11] Printrun: Pure Python 3d printing host software n.d. https://www.pronterface.com/ (accessed June 18, 2019).

[12] Achilleos E, Georgiou GC, Hatzikiriakos SG. On numerical simulations of polymer extrusion instabilities. *Appl Rheol* 2002;**12**:88–104.

[13] Afonso AM, Oliveira PJ, Pinho FT, Alves MA. Dynamics of high-Deborah-number entry flows: A numerical study. *J Fluid Mech* 2011;**677**:272–304. doi:10.1017/jfm.2011.84.